Synthesis Functional Poly(carbonate-*b*-ester) Copolymers and Micellar Characterizations

Fang-Chyou Chiu,[1] Chia-Sheng Lai,[1] Ren-Shen Lee[2]

[1]*Department of Chemical Engineering and Material, Chang Gung University, Taoyuan, Taiwan, Republic of China*
[2]*Center of General Education, Chang Gung University, Taoyuan, Taiwan, Republic of China*

Received 13 December 2006; accepted 20 February 2007
DOI 10.1002/app.26454
Published online 11 June 2007 in Wiley InterScience (www.interscience.wiley.com).

ABSTRACT: Functional poly(carbonate-*b*-ester)s were synthesized in buck by ring-opening polymerization of the carbonate (TMC, MBC, or BMC) with *tert*-butyl *N*-(2-hydroxyethyl) carbamate as an initiator, and then with ε-CL (or ε-BCL) comonomer. Subsequently, the PMMC-*b*-PCL with pendent carboxyl groups and the PTMC-*b*-PHCL with pendent hydroxyl groups were obtained by catalytic debenzylation. DSC analysis indicated that only one T_g at an intermediate temperature the T_gs of the two polymer blocks. A decrease T_g was observed when an increase contents of ε-CL incorporated into the copolymers. In contrast, two increased T_ms were observed with increasing PCL content. The block copolymers formed micelle in aqueous phase with critical micelle concentrations (cmcs) in the range of 2.23–14.6 mg/L and with the mean hydrodynamic diameters in the range of 100–280 nm, depending on the composition of copolymers. The drug entrapment efficiency and hydrolytic degradation behavior of micelle were also evaluated. © 2007 Wiley Periodicals, Inc. J Appl Polym Sci 106: 283–292, 2007

Key words: functional poly(carbonate-*b*-ester); micelles; biodegradation

INTRODUCTION

For the last two decades, aliphatic polycarbonates have been widely investigated because of their biodegradability, biocompatibility, and nontoxicity. However, most of them are hydrophobic and are slow to degrade. For example, the *in vitro* degradation of poly(1,3-dioxane-2-one) (PTMC) in pH 7.4 phosphate buffer solution (PBS) after 30 weeks at 37°C resulted in only 9 wt % loss and 7% molecular weight decrease, which was approximately 20 times less than that of the aliphatic ester poly(caprolactone) (PCL).[1] To improve their hydrophilicity, biodegradability, and mechanical properties, much effort has been devoted to the design and synthesis of new aliphatic polycarbonates having functional pendent groups,[2] such as OH,[3–6] NH_2,[7] COOH,[8–10] and COOR[11–13] groups, or copolymer with hydrophilicity segments.

PCL is either one of the most important biodegradable polymers for its high degradability, biocompatibility, good permeability to drugs, and nontoxicity.[14] However, PCL has a slow degradation rate because of its hydrophobicity and high crystallinity, which have a large negative influence on its applications. Modification via copolymerization is one of effective way to prepare the materials with desirable properties.

Poly(ethylene oxide-*b*-ε-caprolactone) has attracted much attention, because this kind of polyester–polyether-type block copolymer has a superior amphiphilic property as compared with the parent PCL homopolymer.[15–17] Block copolymer of ε-CL with vinyl pyrrolidone also exhibits amphiphilic property by forming micelles of 30–80 nm.[18] Copolymerization of ε-CL with other cyclic ester monomer,[19–24] such as lactide, carbonate, and others, improves the crystallinity and biodegradation of PCL. Recently, functionalized cyclic monomers such as NCA's of amino acids,[25] (3*S*)-[(benzoxylcarbonyl) methyl]-morpholine-2,5-dione,[26] and ε-CLs-bearing carboxyl[27] or hydroxyl[28] groups have been used as the comonomers to prepare functionalized poly(ε-CL)s. They are expected to have enhanced chemical reactivity and to facilitate further modifications to improve the biocompatibility and bioaffinity. To our knowledge, synthesis of the block copolymer of carboxyl-bearing cyclic carbonates with ε-CL only a few was reported in literature.[29] But, its properties in an aqueous solution have never been reported.

Therefore, in this paper, functionalized poly(carbonate-*b*-ester)s were synthesized from trimethylene carbonate bearing the benzylcarboxylate or the benzyloxyl groups and ε-CL with benzyloxyl groups via

Correspondence to: R.-S. Lee (shen21@mail.cgu.edu.tw).
Contract grant sponsor: National Science Council; contract grant number: NSC 95-2221-E-182-025.
Contract grant sponsor: Chang Gung University; contract grant number: BMRP 123.

the ring-opening polymerization in the presence of the *tert*-butyl *N*-(2-hydroxyethyl)carbamate as an initiator. After catalytic hydrogenation, the pendent benzyl ester or benzyloxy groups were converted to carboxyl or hydroxyl groups. The physicochemical properties of block copolymers in an aqueous phase were examined by fluorescence spectroscopy, dynamic light scattering (DLS), and transmission electron microscopy (TEM).

EXPERIMENTAL

Materials

tert-Butyl *N*-(2-hydroxyethyl)carbamate (Aldrich), pyrene (Aldrich), antitriptyline hydrochloride (AM) (Aldrich), and stannous octoate ($SnOct_2$) (Strem) were used as received. ε-CL (Aldrich) was dried and vacuum distilled over calcium hydride. Trimethylene carbonate (TMC), 5-methyl-5-benzyloxycarbonyl-propylene carbonate (MBC), 5-benzyloxy-trimethylene carbonate (BMC), and 4-benzyloxy-ε-caprolactone (ε-BCL) were prepared according to the reported method.[3,27,29,30] Organic solvents such as tetrahydrofuran (THF), methanol, chloroform, and *n*-hexane were HPLC grade and were used without further purification. Ultrapure water was used by purifying (Milli-Q Plus, Waters).

Characterization

^1H and ^{13}C NMR spectra were obtained on a Bruker WB/DMX-500 spectrometer at 500 MHz, with chloroform (δ 7.24 or 76.9 ppm) as an internal standard in chloroform-*d* ($CDCl_3$). A thermal analysis of the polymer was performed on a DuPont 9900 system that consisted of DSC. The heating rate was 20°C/min. T_gs were read at the middle of the change in the heat capacity and were taken from the second heating scan after quick cooling. Number- and weight-average molecular weights (M_n and M_w, respectively) of the polymer were determining by a GPC system. It was carried out on a Jasco HPLC system equipped with a model PU-2031 refractive-index detector, and Jordi Gel DVB columns with pore sizes of 10^2, 500, and 10^3 Å. Chloroform was used as an eluent at a flow rate of 0.5 mL/min. Polystyrene standards with a low dispersity (Polymer Sciences) were used to generate a calibration curve. Data were recorded and manipulated using a Windows-based software package (Scientific Information Service).

The matrix-assisted laser desorption/ionization time-of-flight (MALDI-TOF) mass spectrometry analyses were performed on an Ultraflex™ MALDI-TOF/TOF mass spectrometer (Bruker Daltonik GmbH, Bremen, Germany). The mass range from 600 to 7000 *m/z* was recorded in positive-ion reflectron mode. Typically, 0.5 μL of the sample was dried on a target plate (600-μm AnchorChip, Bruker Daltonics) and cocrystallized with 0.3 μL of a matrix solution (2 mg/mL α-cyano-4-hydroxycinnamic acid in 80% acetonitrile and 1% trifluoroacetic acid) containing 3 fmol purified peptides from antibovine albumin (BSA) (clip 161–167, *m/z* 927.49), α-s2-casein (clip 130–140, *m/z* 1195.68) and adrenocorticotropic hormone (ACTH) (clip18–39, *m/z* 2465.20). The samples were then irradiated using a nitrogen laser (337 nm) with an accelerating voltage of 25 kV and a delay of 200 ns. Typically, data from 200 to 500 laser shots were accumulated to get acceptable quality. The spectra were calibrated internally with the introduced peptides.

UV–vis spectra were obtained with a Jasco V-550 spectrophotometer. The pyrene fluorescence spectra were recorded on a Hitachi F-4500 spectrofluorometer. Square quartz cells (1.0×1.0 cm^2) were used. For fluorescence excitation spectra, the detection wavelength λ_{em} was set at 390 nm.

Preparation of macroinitiators

Hydroxyl-terminated functional PTMC was prepared with *tert*-butyl *N*-(2-hydroxyethyl)carbamate initiating the ring-opening polymerization of functional carbonate. In all, 0.765 mmol of *tert*-butyl *N*-(2-hydroxyethyl)carbamate and 7.65 mmol of carbonate (TMC, MBC, or BMC) was polymerized in the melt at 110°C (or 140°C) for 8 h. The crude polymers were dissolved in $CHCl_3$, microfiltered, and then precipitated into excess CH_3OH with stirring. After purification, the macroinitiators were dried *in vacuo* at 50°C for 24 h. M_ns and thermal properties of macroinitiators are shown in Table I. Representative ^1H NMR spectrum of PBMC is shown in Figure 1(A).

Synthesis of functional PTMC-*b*-PCL diblock copolymers

All glass equipments were dried using oven and handled under a dry nitrogen stream. The typical process for the polymerization to give functional PBMC-*b*-PCL is as follows. PBMC (M_n = 2890 g/mol) (0.62 g, 0.21 mmol) and ε-CL (2.45 g, 21.49 mmol) were introduced into a flask and heated under a dry nitrogen stream to homogenize. Then, 50 mg (1.5 wt %) of $SnOct_2$ was administered into the flask. The flask was purged with nitrogen and reacted at 140°C for 8 h. The resulting product was dissolved in $CHCl_3$, and then precipitated into excess ether with stirring. The purified polymer was dried *in vacuo* at 50°C for 24 h and analyzed. Representative ^1H and ^{13}C NMR spectra of the PBMC-*b*-PCL64 are shown in Figures 1(B) and 3.

TABLE I
Results of Macroinitiator Prepared by Ring-Opening Polymerization of Cyclic Carbonate (TMC, MBC, and BMC) With Initiator *tert*-Butyl *N*-(2-hydroxyethyl)-carbamate[a]

Macroinitiator	Reaction temperature (°C)	$M_{n,\text{th}}$[b]	$M_{n,\text{MALDI}}$[c]	$M_{n,\text{GPC}}$[d]	M_w/M_n[d]	T_g (°C)[e]
PTMC	110	1180	1184	2130	2.14	−27
PMBC	140	2660	2613	2580	1.91	1
PBMC	140	2240	2701	2890	1.34	−3

[a] The polymerization was carried out with the molar ratio [M]/[I] = 10 at 110°C (or 140°C) for 8 h.
[b] $M_{n,\text{th}} = M_{\text{initiator}} + M_{\text{R-TMC}} \times [\text{M}]/[\text{I}]$ (where $M_{\text{initiator}}$ is the molecular weight of *tert*-butyl *N*-(2-hydroxyethyl)carbamate, $M_{\text{R-TMC}}$ is the molecular weight of functional R-TMC, [M] is the monomer molarity concentration, and [I] is the initiator molarity concentration).
[c] Determined using MALDI-TOF mass spectrum.
[d] Determined using GPC.
[e] Determined from DSC thermograms.

Measurements of fluorescence spectroscopy

To prove the formation of the micelles, fluorescence measurements were carried out using pyrene as a probe.[31] Fluorescence spectra of pyrene in aqueous solution were recorded at room temperature on a fluorescence spectrophotometer. The sample solutions were prepared by first adding known amounts of pyrene in acetone to a series of flasks. After the acetone had evaporated completely, measured amounts of micelle solutions with various concentrations of PBMC-*b*-PCL64 were added to each of the flasks and mixed by vortexing. The concentration of pyrene in the final solutions was $6.1 \times 10^{-7}M$. The flasks were allowed to stand overnight at room temperature to equilibrate the pyrene and the micelles. The emission wavelength was 390 nm for excitation spectra.

Measurements of size and size distribution

The size distribution of micelles were estimated by a DLS using a Particle-Size Analyzer (Zatasizer nano ZS) at 20°C. The intensity of a scattered light was detected at 90° to an incident beam. Measurements were made after the aqueous micellar solution (C = 0.3 g/L) was filtered with a microfilter having an average pore size of 0.2 (Advantec MFS, USA). An average size distribution of aqueous micellar solution was determined based on CONTIN programs of Provencher and Hendrixs.[32]

Observation of transmission electron microscope

The morphology of the micelles was observed by TEM (JEM 1200-EXII). Drops of micelle solution (C = 0.3 g/L) were placed on a carbon film coated on a copper grid, and then were dried at room temperature. Observation was done at an accelerating voltage of 100 kV.

Determination of drug entrapment efficiency

Using oil-in-water solvent evaporation, functional PTMC-*b*-PCL (10-fold CMC value) was dissolved in 6 mL methylene chloride followed by adding AM with various weight ratios to polymer (0.1/1 to 1/1) served as model drug. The solution was added dropwise to 50 mL distilled water containing 1 wt % poly(vinyl alcohol) under vigorous stirring. Droplet size was reduced by sonication. The emulsion was stirred at ambient temperature for overnight to evaporate methylene chloride. The aggregated AM-loaded micelles were removed by centrifugation (3000 rpm × 30 min). Then, the micelles solution was lyophilized by concentration. The unloaded AM was eliminated by washing three times with distilled water because of the solubility of AM in water is very large than block copolymer and micelle. The micelles were obtained by vacuum-dried. A weighed amount of micelle was disrupted by an addition of acetonitrile (10 mL). Drug content was assayed spectrophotometrically at 240 nm using a Diode Array UV–vis spectrophotometer. The drug entrapment efficiency (DEE) was presented by following equation:

$$\text{Drug entrapment efficiency (\%)} = (\text{Weight of drug in micelles}/\text{Weight of drug fed initially}) \times 100$$

In vitro degradation

In vitro degradation of about 50 mg of copolymer thin pellet was performed in 5 mL PBS (0.067*M*, pH 7.4) at 37°C, and the buffer solution was changed every 2 days. At specific time intervals, the specimen was removed, washed with distilled water, lyophilized, weighed, and analyzed by GPC. The degree of degradation (%) = $100(D_0 - D)/D_0$, where D_0 is the weight of copolymer before degradation, and D is the weight of copolymer after degradation for a certain period.

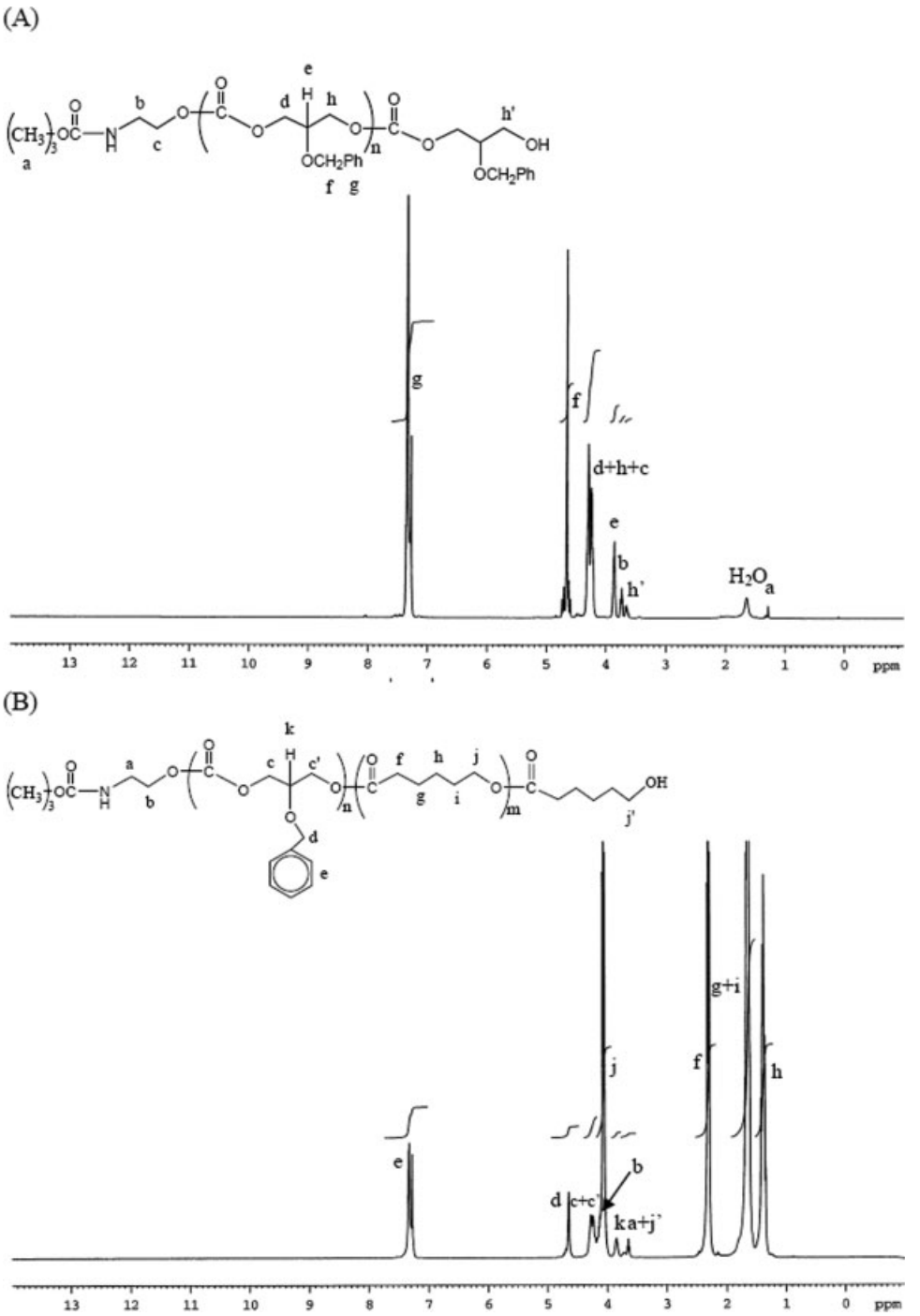

Figure 1 Representative ^{1}H NMR spectra of (A) macroinitiator PBMC with hydroxyl end group, and (B) diblock copolymer PBMC-*b*-PCL64 in $CDCl_3$.

RESULTS AND DISCUSSIONS

Synthesis and characterization of functional PTMC-*b*-PCL copolymers

Various functional PTMC-*b*-PCL diblock copolymers were obtained via the ring-opening polymerization of ε-CL (or ε-BCL) with hydroxyl-terminated macroinitiator (PTMC, PMBC or PBMC). The synthesis of functional PTMC-*b*-PCL block copolymers is illustrated in Scheme 1. First, the hydroxyl-terminated PTMC, PMBC, and PBMC were prepared by the ring-opening homopolymerization of TMC, MBC, and BMC with initiator *tert*-butyl *N*-(2-hydroxyethyl)carbamate (with the molar ratio 10/1) without catalyst in buck at 110°C for 8 h, respectively. The results of the polymerization are compiled in Table I. The number-average molecular weight of macroinitiators were determined by MALDI-TOF ($M_{n,\mathrm{MALDI}}$)

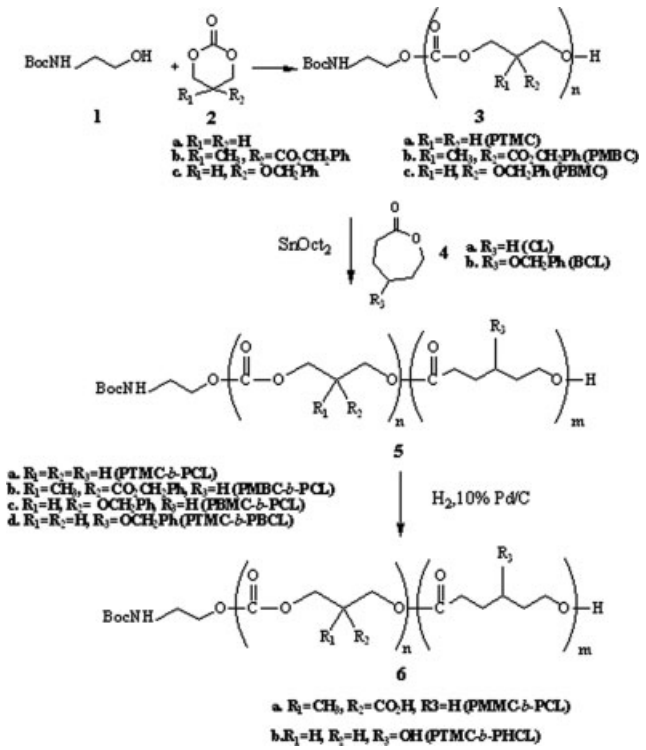

Scheme 1 Synthesis of the functional PTMC-*b*-PCL diblock copolymers.

in agreement with $M_{n,th}$, and $M_{n,GPC}$ except the PTMC. $M_{n,GPC}$ of PTMC is larger than its $M_{n,th}$. This may be due to the PTMC aggregation in GPC (CH_3Cl) solution.[33]

The hydroxyl group of macroinitiator was used as the initiation site for the ring-opening polymerization of ε-CL (or ε-BCL) with $SnOct_2$ as the catalyst to produce the functional PTMC-*b*-PCL diblock copolymers. To find the optimum copolymerization condition, we investigated the effects of the reaction time and temperature on M_n. The results are shown in Figure 2. M_n increased when the reaction time increased and closed to $M_{n,th}$ for 24 h. If the reaction temperature was decreased to 110°C, a lower M_n (5950 g/mol) was observed. Table II summarizes the results for the block copolymerization of macroinitiator (PTMC, PMBC, or PBMC) with ε-CL (or ε-BCL). With the fixed PTMC macroinitiator, copolymers with different compositions were prepared by changes in the monomer ε-CL feed ratios for $SnOct_2$-catalyzed polymerization at 140°C for 24 h. The M_n values of the obtained block copolymers increased with an increase in the molar ratios of ε-CL to PTMC in the feed. The M_n values of the copolymers increased from 7590 to 12,860 g/mol, with M_w/M_n between 1.39 and 1.62; the molar ratios of ε-CL to PTMC in the feed increased from 30 to 100. The molar ratios of the compositions in the block copolymers were analyzed with ^{1}H NMR. The amount of the monomer incorporated into the copolymer could be calculated from a comparison of the integral area of the absorption peaks (δ = 1.95–1.99 ppm) of the methylene protons (C_5) of PTMC with the absorption peaks (δ = 2.27–2.31 ppm) of the methylene protons (C_2) of PCL. The conversion of the copolymerization of the monomers was slightly lower than the corresponding feeds. However, there was good agreement between the assumed molecular weight [theoretical number-average molecular weight ($M_{n,th}$)] and the GPC-determined number-average molecular weight ($M_{n,GPC}$). According to ^{1}H NMR spectroscopy, the PMBC or PBMC as a macroinitiator, the ε-CL copolymerization with PMBC or PBMC is slower than with PTMC. Similarly, the substituted lactones (ε-BCL) copolymerized significantly slower than do ε-CL.[28] The fact is attributed to the steric hindrance, resulted the polymerization slow down.

Typical ^{1}H NMR spectra and their peak assignment of macroinitiator PBMC with a molar ratio of [BMC]/[initiator] = 10 and the block copolymer PBMC-*b*-PCL64 with a molar ratio of [ε-CL]/[PBMC] = 64 were shown in Figure 1. The typical signals of the main chain of the PBMC blocks and the PCL blocks are found to be in agreement with those reported in Refs. 29 and 34. There are several additional peaks, more or less overlapped, resulting from the incorporation of *tert*-butyl *N*-(2-hydroxyethyl)carbamate at δ = 1.29 ($(CH_3)_3C$—), 3.63 (—N—CH_2—), and 4.15 (—O—CH_2—) ppm.

The ^{13}C NMR spectrum of PBMC-*b*-PCL64 diblock copolymer is shown in Figure 3. The typical signals of the PCL blocks are seen at δ = 24.5, 25.3, 28.1, and 33.7 (C_{k-n}, the methylene carbons), 63.9 (C_0, the methylene carbon), and 173.4 (C_j, ester carbonyl) ppm, respectively. The adsorption peaks of PBMC blocks are shown at δ = 66.1 (C_h, the benzyl carbon), 67.9 (C_p, the methine carbon), 72.1 ($C_{g+g'}$, the methyl-

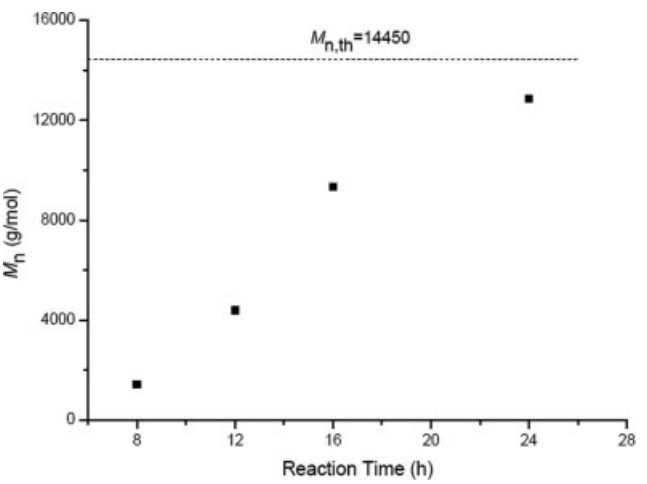

Figure 2 The effect of reaction time on the M_n of PTMC-*b*-PCL (conditions: the molar ratio of [ε-CL]/[PTMC] = 100 with $SnOct_2$ (1.5 wt %) as a catalyst at 140°C).

TABLE II
Results of the Block Copolymerization of Functional ε-Caprolactone Initiated With Hydroxyl-Terminated Macroinitiator in Bulk at 140°C With 1.5 wt % $SnOct_2$ as the Catalyst for 24 h

Copolymer	Molar ratio of monomer **4** over macroinitiator **3** in feed [4]/[3]	[4]/[3] molar ratio[a]	$M_{n,th}$[b]	$M_{n,NMR}$[a]	$M_{n,GPC}$[c]	M_w/M_n[c]	T_g (°C)[d]	T_{m1} (°C)[d]	T_{m2} (°C)[d]
PTMC-*b*-PCL16	30/1	16/1	6,470	2,840	7,590	1.39	−41	38	47
PTMC-*b*-PCL44	60/1	44/1	9,890	6,030	8,290	1.39	−47	43	48
PTMC-*b*-PCL65	80/1	65/1	12,170	8,420	10,470	1.62	−49	42	49
PTMC-*b*-PCL85	100/1	85/1	14,450	10,700	12,860	1.59	−53	48	52
PMBC-*b*-PCL79	100/1	79/1	13,980		13,330	1.32	−43	49	56
PBMC-*b*-PCL64	100/1	64/1	14,290	8,980	13,740	1.41	−48	45	52
PTMC-*b*-PBCL82	100/1	82/1	24,170	19,050	15,370	1.64	−21		
PTMC-*b*-PHCL82	100/1		14,270		12,280	2.29	−47		
PMMC-*b*-PCL79	100/1		12,580		10,810	1.65	−64	43	51

[a] Determined using ^{1}H NMR spectroscopy.
[b] $M_{n,th} = M_{n,macroinitiator} + M_{4\text{-R-}\varepsilon\text{-CL}} \times [M]/[I]$ (where $M_{n,macroinitiator}$ is the number-average molecular weight of macroinitiator, $M_{4\text{-R-}\varepsilon\text{-CL}}$ is the molecular weight of functional 4-R-ε-CL, [M] is the monomer molarity concentration, and [I] is the macroinitiator molarity concentration).
[c] Determined using GPC.
[d] Determined from DSC thermograms.

ene carbons), 127.6 and 128.4 (C_i, the phenyl carbons), and 154.5 (C_f, carbonate carbonyl) ppm, respectively. Some additional weak peaks at δ = 25.5, 32.1, 62.4, and 137.5 ppm which belong to the end groups of initiator are also found.

The thermal behaviors of the block copolymers and DSC curves of PTMC-*b*-PCL are shown in Table II and Figure 4, respectively. According to DSC, with an increase in the contents of ε-CL incorporated into the copolymers, a decrease in T_g of the copolymers was observed. The values of T_g decreased from −41 to −53°C when the molar ratio of [ε-CL]/[PTMC] increased from 16 to 85. This is due to the fact that ε-CL is a soft component, when a larger amount of flexible linkages was incorporated into the macromolecular backbone there was a decrease in T_g. However, only one T_g at an intermediate temperature between the T_gs of the two polymer blocks (T_g = −15°C for PTMC; T_g = −61°C for PCL) was observed. This is due to the two polymeric segments are miscible in bulk.[35] Similarly exchanging the macroinitiator PMBC or PBMC, the functional copolymer exhibited only one T_g that higher than PTMC copolymer. Two increased T_m were observed in all PTMC-*b*-PCLs from 38 to 48°C, and from 47 to 52°C, increasing with increasing PCL content. However, only the PCL is the crystalline component in the block copolymer. The existence of two melting temperature very close together might be the primary and secondary crystallization of PCL. But, the T_m of PTMC-*b*-PCLs is lower than that of the homopolymer PCL (58.3°C). It implied that the crystallinity

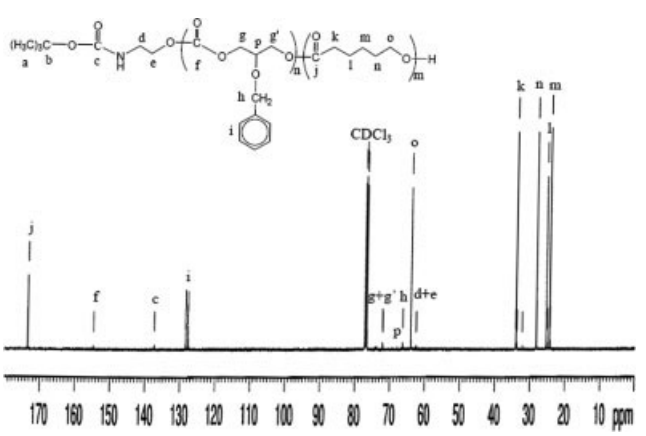

Figure 3 ^{13}C NMR spectrum of PBMC-*b*-PCL64 diblock copolymer in $CDCl_3$.

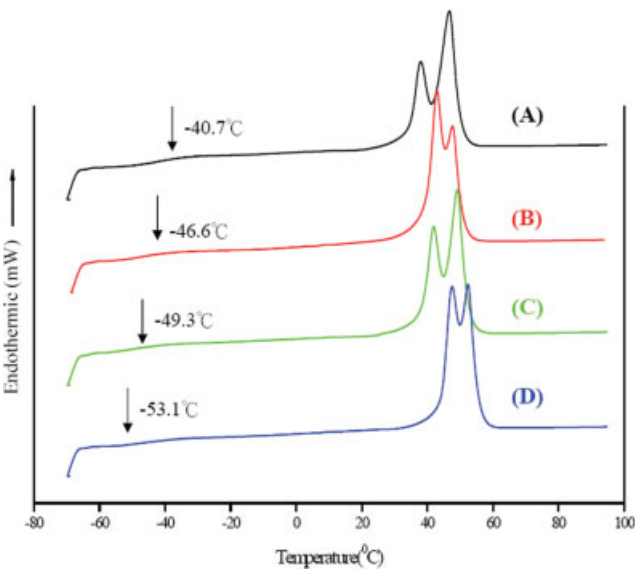

Figure 4 DSC curves of PTMC-*b*-PCL with the molar ratio [ε-CL]/[PTMC] (A) 16/1, (B) 44/1, (C) 65/1, and (D) 85/1 for second run.

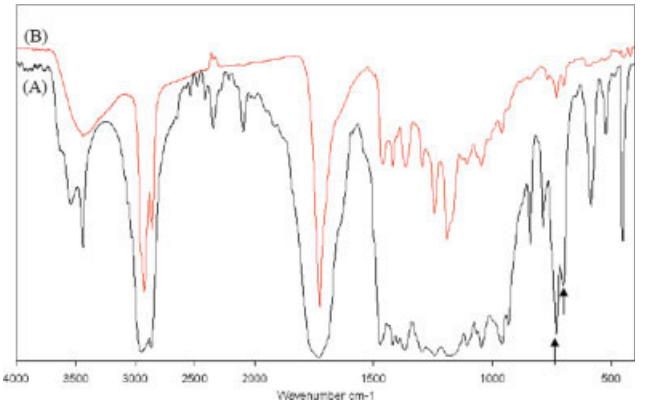

Figure 5 IR spectra of PMBC-*b*-PCL79 (A) before and (B) after deprotection.

and crystal perfectness of the PCL blocks were lowered due to the presence of PTMC segments. With the same macroinitiator PTMC, if BCL was incorporated into the copolymers, an increase in T_g was observed but not in T_m. This demonstrated that PBCL is harder and less crystalline than PCL (PTMC-*b*-PBCL82, and PTMC-*b*-PCL85).

Deprotection

The benzyl protecting groups of the PMBC-*b*-PCL79 and PTMC-*b*-PBCL82 were easily removed to get carboxyl-substituted block copolymers PMMC-*b*-PCL79 and hydroxyl-substituted block copolymers PTMC-*b*-PHCL82 by catalytic hydrogenolysis over Pd/C (10%) in THF/CH_3OH. Notably, to avoid the inactivation of the catalyst due to polymer wrapping, the polymer must be completely dissolved in THF. Then, the polymer solution was added to the solution of Pd/C suspension in CH_3OH. The debenzylation of PMBC-*b*-PCL79 and PTMC-*b*-PBCL82 were performed under 1.0 atm H_2 atmosphere at 50°C for 48 h. All benzyl groups were almost removed, as evident from the lowering of the δ_{CH} vibrations of benzyl group at 751 and 698 cm^{-1} in the FTIR spectra (Fig. 5). Figure 6 shows the typical GPC curves of deprotecting diblock copolymer PMMC-*b*-PCL79 with pendent carboxyl groups as compared with the original copolymer PMBC-*b*-PCL79. The peak shifted toward a slight smaller molecular weight region and little broad in the molecular weight distribution in comparison with the peak of the original copolymer. After debenzylation, the T_g and T_ms of PMMC-*b*-PCL79 are lower than that of its parent polymer PMBC-*b*-PCL79. This was attributed to the formation of the COOH groups and less steric hindrance in PMMC-*b*-PCL79. The hydrogen bonds could be formed not only between the carboxyl groups in PMMC segments, but also between the carboxyl groups in PMMC blocks and the ester groups in PCL blocks. These latter interblock interactions, especially the intermolecular hydrogen-bonding hampered the crystallization of PCL segments. Similar result, a decreased T_g, was observed for PTMC-*b*-PHCL82.

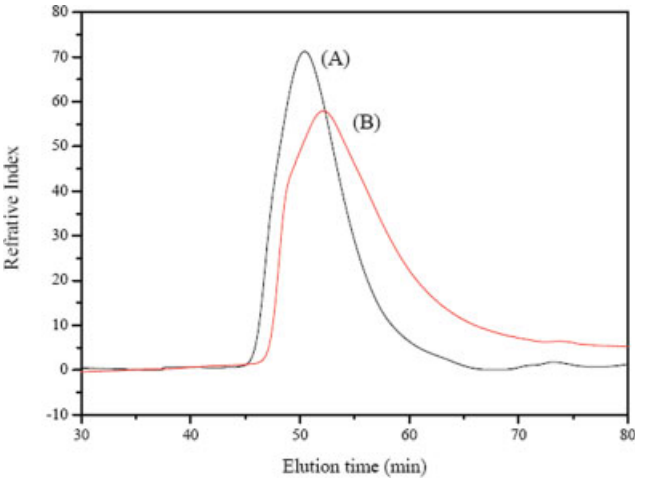

Figure 6 GPC curves of (A) PMBC-*b*-PCL79 and (B) deprotected of PMBC-*b*-PCL79 (PMMC-*b*-PCL79).

Micelles of block copolymers

The critical micelle concentration (CMC) of the block copolymers in an aqueous phase were determined by a fluorescence technique using pyrene as a probe. Typical excitation spectra of pyrene in the PBMC-*b*-PCL64 solution with various concentrations are shown in Figure 7. As it can be seen, the fluorescence intensity increases with increasing the concentration of PBMC-*b*-PCL64. The characteristic feature of pyrene excitation spectra, a red shift of the (0, 0) band from 335 to 338 nm upon pyrene partition into micellar hydrophobic core, was used to determine the CMC values of block copolymers. Figure 8 shows the intensity ratios of the (0, 0) band to the (0, 2) band (I_{max}/I_{min}) of pyrene excitation spectra versus the logarithm of PTMC-*b*-PCL85, PMBC-*b*-

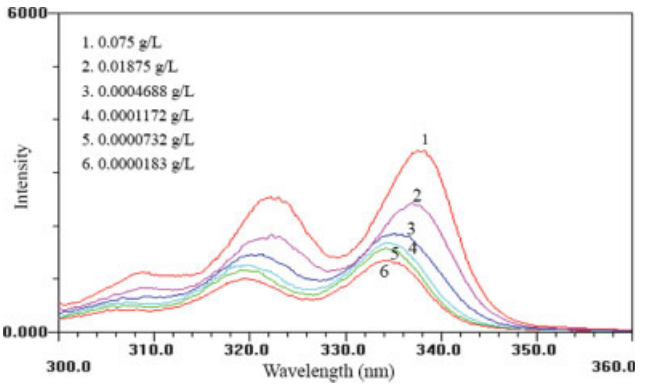

Figure 7 Excitation spectra of pyrene as a function of PBMC-*b*-PCL64 concentration in deionized water, λ_{em} = 390 nm.

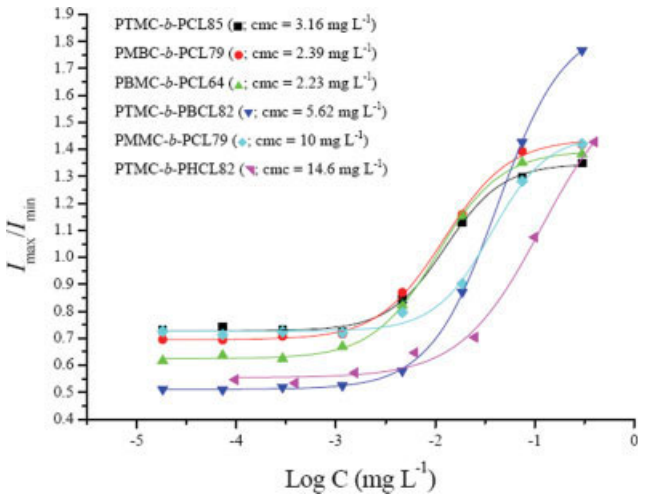

Figure 8 Plot of the I_{max}/I_{min} intensity ratio (from pyrene excitation spectra; pyrene concentration = $6.1 \times 10^{-7}M$) versus the logarithm of the concentration (log *C*).

PCL79, PBMC-*b*-PCL64, PTMC-*b*-PBCL82, PMMC-*b*-PCL79, and PTMC-*b*-PHCL82 block copolymers concentration. The CMC was determined from the intersection of straight line segments, drawn through the points at the lowest polymer concentrations, which lie on a nearly horizontal line, with that going through the points on the rapidly rising part of the plot. The CMC values of the block copolymers were 3.16 mg/L (PTMC-*b*-PCL85), 2.39 mg/L (PMBC-*b*-PCL79), 2.23 mg/L (PBMC-*b*-PCL64), 5.62 mg/L (PTMC-*b*-PBCL82), 10.0 mg/L (PMMC-*b*-PCL64), and 14.6 mg/L (PTMC-*b*-PHCL82), respectively, depending on the block composition. The length and steric hindrance of hydrophobic segment increased, the CMC values increased. This may reflect the enhanced hydrophobic block in the core due to the PCL or PBCL linkages and contributions of pyrene near the hydrophobic interface of the core and prefer partition into the hydrophobic microdomains. After debenzylation, the CMC values increased remarkably from 2.39 to 10.0 mg/L for PMMC-*b*-PCL64, and from 5.62 to 14.6 mg/L for PTMC-*b*-PHCL82, respectively. This may be due to the difference of hydrophilic and hydrophobic segment increase, enhance the aqueous solubility of polymer.

The mean hydrodynamic diameters of micelles from DLS were in the range of 100–280 nm, and size distribution showed a monodisperse unimodel pattern as shown in Figure 9. The results indicated that the micelles size were dependent on the composition of polymer. Polymers with longer hydrophobic blocks or with larger pendent groups in polymer backbone show a higher tendency to form larger aggregates. Therefore, the micelles size in water decreased when the hydrophilicity of polymer increased after debenzylation, in agreement with the literature.[35] Also, the morphology of the micelles was shown in Figure 10. Almost spherical micelles were observed for functional PTMC-*b*-PCL, except the PBMC-*b*-PCL82 appear the core–shell shape.

Drug entrapment efficiency

An amount of AM incorporated into functional PTMC-*b*-PCL micelles was calculated by the difference in weight ratio of AM in nanosphere to the preweighed AM-loaded micelles, which was calculated by UV absorbance after removing free AM and AM bounded on the surface of micelles by sonication with distillated water. The amount of AM introduced into the micelle by controlling the weight ratio between polymer and drug is shown in Table III. The DEE increased with the weight ratio of drug to polymer. For example, in the case of PTMC-*b*-PCL85, the feed weight ratio of AM to polymer increase from 0.1 to 1, the DEE increased from 11.6% to 49.4%. Also, the DEEs depending on composition of block polymer were described. For different composition copolymers PMBC-*b*-PCL79, PBMC-*b*-PCL64, and PTMC-*b*-PBCL82, the DEEs are 49.8, 37.3, and 24.9%, respectively. After debenzylation, increased DEE was observed 54.6% (PMMC-*b*-PCL79). This effect is rather complicated and can be affected by many factors, such as molecular weight, the ratio of hydrophobic segment to hydrophilic segment, crystallinity, and so on. So no regular change with respect to DEE is found (see Table III).

Preliminary *in vitro* degradation study

As a model of biodegradation, the *in vitro* degradation of functional PTMC-*b*-PCLs was evaluated from the change in the molecular weight versus the

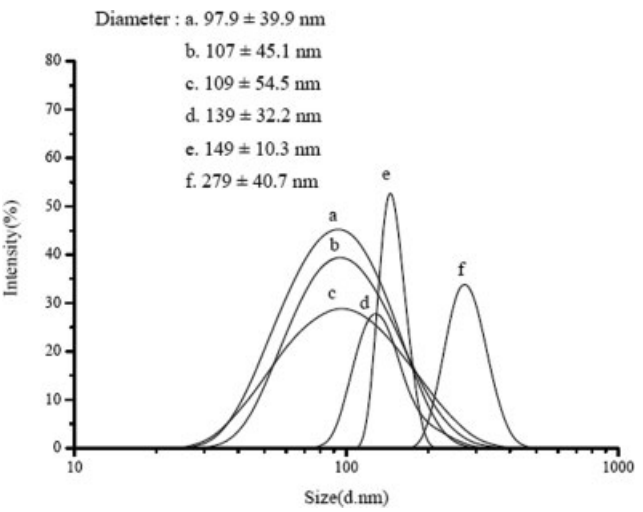

Figure 9 Effect of the composition of copolymers (a) PMMC-*b*-PCL79, (b) PTMC-*b*-PHCL82, (c) PMBC-*b*-PCL79, (d) PTMC-*b*-PBCL82, (e) PTMC-*b*-PCL85, and (f) PBMC-*b*-PCL64 on the size of micelle particles.

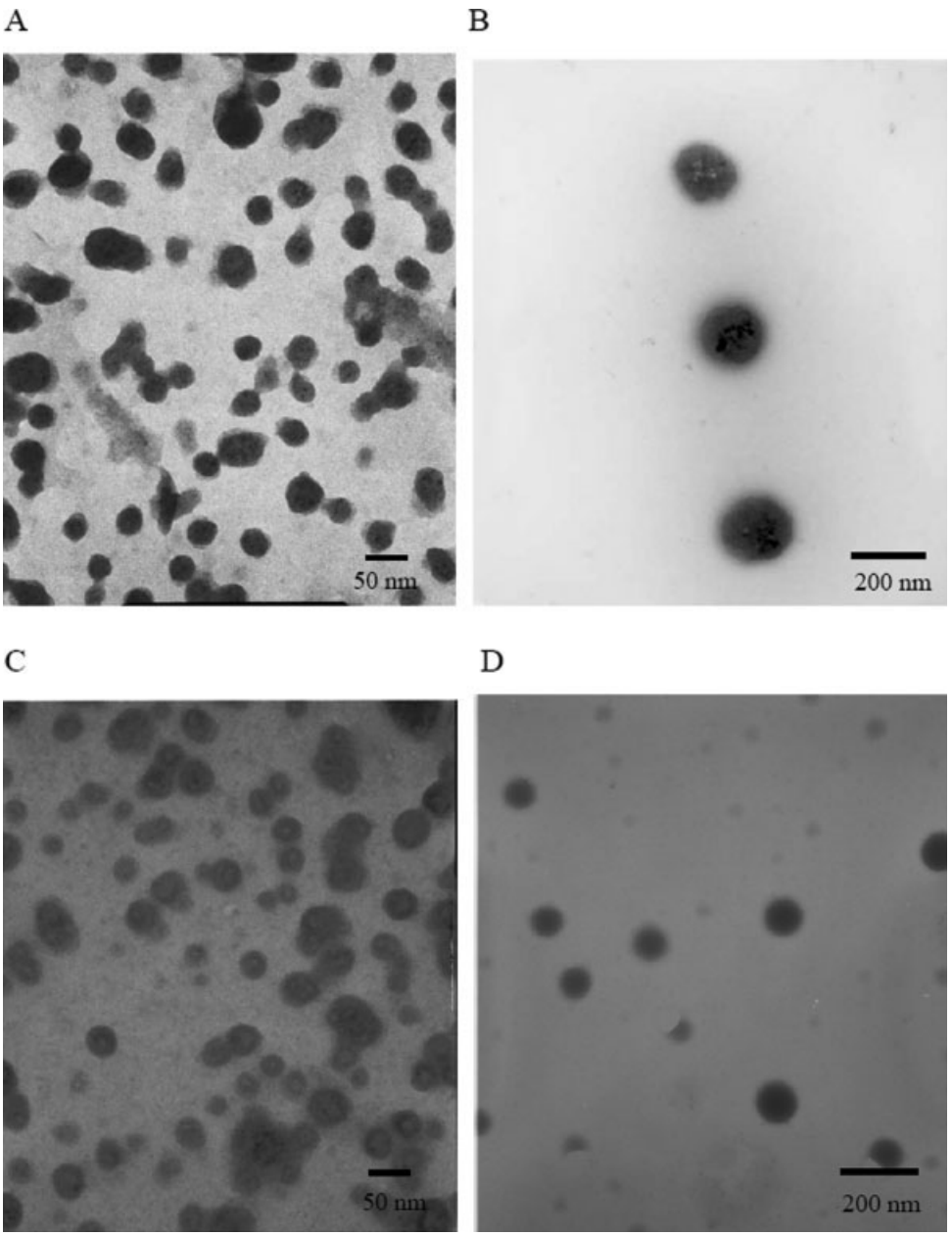

Figure 10 TEM photograph of the micelles formed by (A) PTMC-*b*-PCL85, (B) PMBC-*b*-PCL79, (C) PBMC-*b*-PCL82, and (D) PMMC-*b*-PCL79.

immersion time. The results are depicted in Figure 11. After 30 days, the M_n decreased from 13,740 to 9330 g/mol for PBMC-*b*-PCL64, from 15,180 to 12,500 g/mol for PMBC-*b*-PCL79, and from 12,860 to 11,060 g/mol for PTMC-*b*-PCL85, respectively. The polydispersity index ($I_p = M_w/M_n$) increased from initial 1.32–1.41 to 1.53–1.71 after immersion for 30 days. The molecular weight loss percentages of the copolymers: 32% (PBMC-*b*-PCL64) > 19.6% (PMBC-*b*-PCL79) > 14% (PTMC-*b*-PCL85). Win increase in the hydrophobic block PCL contents in the copolymers, decreases in molecular weight loss percentages

TABLE III
Drug Entrapment Efficiency of AM-Loaded Functional PTMC-*b*-PCL Diblock Copolymers Micelles

Copolymers	Feed weight ratio copolymer/AM	Drug entrapment efficiency (%)
PTMC-*b*-PCL85	1/0.1	11.6
PTMC-*b*-PCL85	1/0.5	23.0
PTMC-*b*-PCL85	1/1	49.4
PMBC-*b*-PCL79	1/1	49.8
PBMC-*b*-PCL64	1/1	37.3
PTMC-*b*-PBCL82	1/1	24.9
PMMC-*b*-PCL79	1/1	54.6

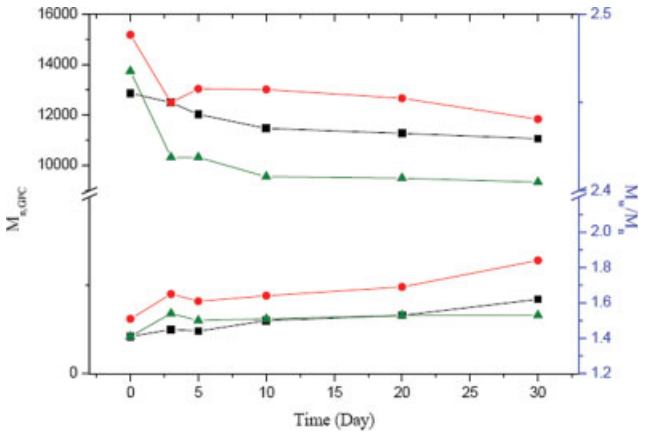

Figure 11 Plot of M_n and M_w/M_n changes of degradation of block copolymers (■) PTMC-*b*-PCL85, (●) PMBC-*b*-PCL79, and (▲) PBMC-*b*-PCL64 in which it was treated in 0.067*M* PBS (pH 7.4) at 37°C.

were observed. The increase in hydrophobic block PCL contents in the copolymers reduces copolymer's hydrophilicity, and thus results in smaller molecular weight losses.

CONCLUSIONS

This work shows that functional poly(carbonate-*b*-ester)s diblock copolymers were successfully synthesized from macroinitiator (PTMC, PMBC, or PBMC) and ε-CL (or ε-BCL) in the presence of $SnOct_2$ as the catalyst. The thermal properties of the diblock copolymers could be controlled by the contents and kinds of ε-CL. The copolymers could form micelles in aqueous solutions, with the CMC dependent on the composition of the copolymers. Using higher hydrophobic components or with larger difference of hydrophilic and hydrophobic segments in the copolymer produced a higher CMC value. DLS experiments showed that the average size of the micelles in the range of 100–280 nm. The morphology of the micelles exhibited a spherical shape, except the PBMC-*b*-PCL82 appear the core-shell. The DEE dependent on the composition of polymer was observed. *In vitro* degradation, using higher hydrophobic block contents produced a lower molecular weight loss percentage.

Presence of the pendent carboxyl or hydroxyl groups on functional poly(carbonate-*b*-ester) is expected to facilitate further modifications of the polymer, such as attaching drug molecules, and short peptides onto the functional groups. Further investigation is in progress and will be reported elsewhere.

The authors are grateful to Kao Chung Shen (Advanced Instrumentation Center, National Taiwan University) for obtaining DSC measurements and the proteomics core lab at Chang Gung University for MALDI-TOF mass spectrometry analysis.

References

1. Zhu, K. J. R.; Hendren, W.; Jensen, K.; Pitt, C. G. Macromolecules 1991, 24, 1736.
2. Ruckenstein, E.; Yuan, Y. M. J Appl Polym Sci 1998, 69, 1429.
3. Wang, X. L.; Zhuo, R. X.; Liu, L. J.; He, F.; Liu, G. J Polym Sci Part A: Polym Chem 2002, 40, 70.
4. Vandenberg, E. J.; Tian, D. Macromolecules 1999, 32, 3613.
5. Ray, W. C., III; Grinstaff, M. W. Macromolecules 2003, 36, 3557.
6. Acemoglu, M.; Bantle, S.; Mindt, T.; Nimmerfall, F. Macromolecules 1995, 28, 3030.
7. Sanda, F.; Kamatani, J.; Endo, T. Macromolecules 2001, 34, 1564.
8. Al-Azemi, T. F.; Bisht, K. S. Macromolecules 1999, 32, 6536.
9. Al-Azemi, T. F.; Harmon, J. P.; Bisht, K. S. Biomacromolecules 2000, 1, 493.
10. Lee, R. S.; Yang, J. M.; Lin, T. F. J Polym Sci Part A: Polym Chem 2004, 42, 2303.
11. Liu, Z. L.; Zhou, Y.; Zhou, R. X. J Polym Sci Part A: Polym Chem 2003, 41, 4001.
12. Mullen, B. D.; Tang, C. N.; Storey, R. F. J Polym Sci Part A: Polym Chem 1978, 2003, 41.
13. Zhou, Y.; Zhuo, R. X.; Liu, Z. L. Macromol Rapid Commun 2005, 26, 1309.
14. Christine, A.; Jeannie, H.; Yu, Y. S.; Dusica, M.; Adi, E. J Controlled Release 2000, 63, 275.
15. Mason, M.; Metters, A.; Bowman, C.; Anseth, K. Macromolecules 2001, 34, 4630.
16. Seretoudi, G.; Bikiaris, D.; Panayiotou, C. Polymer 2002, 43, 5405.
17. Yang-Ho, N.; Yong, H.; Xintao, S.; Yoshihiro, K.; Yoshiharu, D.; Yoshio, I. Biomacromolecules 2002, 3, 1179.
18. Chug, T. W.; Cho, K. Y.; Lee, H. C.; Nah, J. W.; Yeo, J. H.; Akaike, T.; Cho, C. S. Polymer 2004, 45, 1591.
19. Huang, M. H.; Li, S.; Coudane, J.; Vert, M. Macromol Chem Phys 2003, 204, 1994.
20. Jeon, O.; Lee, S. H.; Kim, S. H.; Lee, Y. M.; Kim, Y. H. Macromolecules 2003, 36, 5585.
21. Wahlberg, J.; Persson, P. V.; Olsson, T.; Hedenström, E.; Iversen, T. Biomacromolecules 2003, 4, 1068.
22. Shibasaki, Y.; Sanada, H.; Yokoi, M.; Sanda, F.; Endo, T. Macromolecules 2000, 33, 4316.
23. Agarwal, S.; Naumann, N.; Xie, X. Macromolecules 2003, 35, 7713.
24. Ling, J.; Zhu, W.; Shen, Z. H. Macromolecules 2004, 37, 758.
25. Deng, M.; Wang, R.; Rong, G.; Sun, J.; Zhang, X.; Chen, X.; Jing, X. Biomaterials 2004, 25, 3553.
26. Wang, D.; Feng, J. Macromolecules 1998, 31, 3824.
27. Trollsas, M.; Lee, V. Y.; Mecerreyes, D.; Lowenhielm, P.; Moller, M.; Miller, R. D.; Hedrick, J. L. Macromolecules 2000, 33, 4619.
28. Tian, D.; Halleux, O.; Dubois, P.; Jérome, R. Macromolecules1998,31, 924.
29. Guan, H.; Xie, Z.; Tang, Z.; Xu, X.; Chen, X.; Jing, X. Polymer 2005, 46, 2817.
30. Ariga, T.; Takata, T.; Endo, T. J Polym Sci Part A: Polym Chem 1993, 31, 581.
31. Wilhelm, M.; Zhao, C. L.; Wang, Y.; Xu, R.; Winnik, A. Macromolecules 1991, 24, 1033.
32. Provencher, S. W.; Hendrixs, J. J Phys Chem 1978, 69, 4237.
33. Abbel, R.; Schleuss, T. W.; Frey, H.; Kilbinger, F. M. Macromol Chem Phys 2005, 206, 2067.
34. Zeng, F.; Liu, J.; Allen, C. Biomacromolecules 2004, 5, 1810.
35. Garnier, S.; Laschewsky, A. Macromolecules 2005, 38, 7580.